EXIT Chart Analysis for Iterative Timing Recovery

Piya Kovintavewat and John R. Barry
School of Electrical and Computer Engineering
Georgia Institute of Technology, Atlanta, GA 30332, USA.
{piya, barry}@ece.gatech.edu

Abstract— **Performance analysis of iterative timing recovery schemes, which perform timing recovery, equalization, and error-correction decoding jointly, is difficult because of their complexity. In this paper, we apply the extrinsic information transfer chart (EXIT chart) analysis as a tool to compare and predict their performances. Simulation results indicate that the system performance predicted by the EXIT chart coincides with that obtained by simulating data transmission over a complete iterative receiver, especially when a coded block length is large.**

Index Terms— **Extrinsic information transfer chart (EXIT chart), per-survivor processing (PSP), iterative timing recovery.**

I. Introduction

Timing recovery is the process of synchronizing the sampler with the received analog signal. The quality of synchronization has a dominant impact on overall performance. Iterative error-correction codes (ECCs) allow reliable operation at low signal-to-noise ratio (SNR) because of their large coding gains. This means that timing recovery must also function at low SNR. A conventional receiver performs timing recovery and error-correction decoding separately. Specifically, conventional timing recovery ignores the presence of ECCs. Therefore, it fails to work properly at low SNR.

To improve the performance of conventional timing recovery, two iterative timing recovery schemes, namely *the NBM scheme* [1] and the *per-survivor iterative timing recovery* scheme [2], have been proposed. The NBM scheme is realized by embedding the timing recovery step inside the turbo equalizer [3] so as to perform timing recovery, equalization, and error-correction decoding jointly. Although the NBM scheme outperforms the conventional receiver, it requires a large number of turbo iterations to correct a cycle slip [2]. To improve the performance of the NBM scheme, per-survivor iterative timing recovery has been proposed in [2], which also performs those three tasks jointly. It is realized by first embedding the timing recovery step inside the Bahl, Cocke, Jelinek, and Raviv (BCJR) [4] equalizer based on per-survivor processing (PSP) [5], resulting in a per-survivor BCJR equalizer, denoted as "PSP-BCJR." Then, per-survivor iterative timing recovery iteratively exchanges soft information between PSP-BCJR and a soft-in soft-out (SISO) decoder.

Performance analysis of these two iterative timing recovery schemes is difficult because of their complexity. Accordingly, a time-consuming simulation in terms of bit-error rate (BER) is practically a solution to compare their performances as presented in [2], which indicates that per-survivor iterative timing recovery outperforms the NBM scheme, especially when the timing error is large.

The *extrinsic information transfer chart* (EXIT chart) was proposed by ten Brink [6] as a tool for predicting the convergence behavior of turbo codes [7]. The key idea is that the SISO equalizer and the SISO decoder in an iterative receiver can be modeled as devices mapping the extrinsic information from its input to its output. Because the output of one SISO module is an input to the other SISO module and vice versa, these two transfer characteristics can be plotted in a single diagram with the axes of the decoder transfer characteristic swapped. Furthermore, the exchange of extrinsic information can be visualized as a *system trajectory* between these two transfer characteristics, which can be accurately used to predict the performance of iterative decoding schemes without simulating data transmission on the complete iterative receiver [6].

Recently, the EXIT chart has been employed to analyze the performance of turbo equalization as presented in [8] for the case of a known, time-invariant channel, and in [9] for the adaptive turbo equalization, both assuming that synchronization is perfect. In this paper, we will show that the EXIT chart can also be used to predict the performance of the system with imperfect synchronization or, specifically, the iterative timing recovery scheme. We also validate the use of the EXIT chart instead of BER as a convenient measure to compare the performance of different iterative timing recovery schemes, considering that the BER computation takes a considerable amount of simulation time.

This paper is organized as follows. After describing our system model in Section II, we give simulation setups for generating the EXIT chart of each iterative timing recovery scheme and derive an expression of the predicted BER in Section III. Section IV compares the performance of each scheme. Finally, Section V concludes the paper.

II. System Description

We consider the coded partial response (PR) channel model shown in Fig. 1. The message bits $\{x_k\}$ are encoded to obtain a sequence c_k. The sequence c_k with bit period T passes through the channel corrupted by unknown timing offsets and additive white Gaussian noise (AWGN), $n(t)$, with two-sided power spectral density $N_0/2$, producing

$$s(t) = \sum_k c_k h(t - kT - \tau_k) + n(t), \qquad (1)$$

where $h(t) = p(t) - p(t - 2T)$ is a PR-IV pulse, $p(t) = \sin(\pi t/T)/(\pi t/T)$ is a 0% excess bandwidth pulse, τ_k is the k-th unknown timing offset. We model τ_k as a random walk
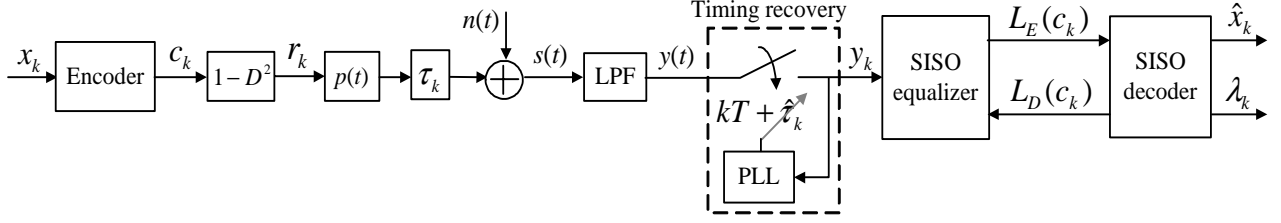
Fig. 1. A channel model with a conventional receiver.

[10] according to $\tau_{k+1} = \tau_k + \mathcal{N}(0, \sigma_w^2)$, where σ_w determines the severity of the timing jitter. The random walk model is chosen because of its simplicity and its ability to represent a variety of channels by changing only one parameter. We also assume perfect acquisition by setting $\tau_0 = 0$.

At the receiver, the readback signal $s(t)$ is filtered by a low-pass filter (LPF), whose impulse response is $p(t)/T$, to eliminate the out-of-band noise, and is then sampled at time $kT + \hat{\tau}_k$, creating

$$y_k = y(kT + \hat{\tau}_k) = \sum_i c_i h(kT + \hat{\tau}_k - iT - \tau_i) + n_k, \quad (2)$$

where $\hat{\tau}_k$ is the receiver's estimate of τ_k, and n_k is an *i.i.d.* zero-mean Gaussian random variable with variance $\sigma_n^2 = N_0/(2T)$, i.e., $n_k \sim \mathcal{N}(0, \sigma_n^2)$.

Conventional timing recovery is based on a phase-locked-loop (PLL) [11]. Because perfect acquisition is assumed and our model has no frequency offset component, the sampling phase offset can then be updated by a first-order PLL according to [11]

$$\hat{\tau}_{k+1} = \hat{\tau}_k + \alpha \{y_k \tilde{r}_{k-1} - y_{k-1} \tilde{r}_k\}, \quad (3)$$

where α is a PLL gain parameter, and $\tilde{r}_k$ is the k-th *soft estimate* of the *channel output* $r_k \in \{0, \pm 2\}$ given by [1]

$$\tilde{r}_k = E[r_k | y_k] = \frac{2 \sinh(2y_k/\sigma_n^2)}{\cosh(2y_k/\sigma_n^2) + e^{2/\sigma_n^2}}. \quad (4)$$

The soft estimate provides a better performance than the *hard estimate* [1], which is obtained by a memoryless three-level quantization of y_k.

In the conventional receiver, conventional timing recovery is followed by the turbo equalizer as depicted in Fig. 1. The SISO equalizer takes the channel observations $\{y_k\}$ and the *a priori* information $L_D(c_k)$ to output the extrinsic information $L_E(c_k)$, which becomes the *a priori* input for the SISO decoder. The SISO decoder outputs soft values $\{\lambda_k\}$ and feeds back the extrinsic information $L_D(c_k) = \lambda_k - L_E(c_k)$ to become the *a priori* input of the SISO equalizer. Note that the variables L and λ are log-likelihood ratios (LLRs).

III. EXIT CHART FOR ITERATIVE TIMING RECOVERY

The analysis tool called the EXIT chart is used to graphically describe the convergence behavior of the iterative decoding scheme by investigating the exchange of mutual information between the equalizer and the decoder. To obtain the EXIT chart, the mutual information at the equalizer output, $I_E^{out} = I(L_E(c_k); c_k)$, and at the decoder output, $I_D^{out} =$

$I(L_D(c_k); c_k)$, is needed, where the mutual information is defined as [6]

$$I(L; C) = \frac{1}{2} \sum_{c \in \{\pm 1\}} \int_{-\infty}^{\infty} p(l|c) \cdot \log_2 \left(\frac{2p(l|c)}{p(l|1) + p(l|-1)} \right) dl, \quad (5)$$

where $p(l|c) = p(l|C = c)$ denotes a probability density function (pdf) of the extrinsic information L given that c was transmitted. The range of $I(L; C)$ is $[0, 1]$, where $I(L; C) = 0$ or $I(L; C) = 1$ means no or perfect knowledge of the transmitted bit c. Equation (5) is evaluated by first calculating the histograms of $c_k L(c_k)$ in order to estimate $p(l|1)$ and $p(l|-1)$. Hence, $I(L; C)$ is obtained by numerically computing the integral in (5).

A. Simulation setup

Fig. 2 shows a simulation setup for generating the mutual information transfer characteristics of the conventional receiver. The *a priori* information is usually modeled as a normal distribution with average value $c_k \sigma_A^2/2$ and variance σ_A^2 [6]. The mutual information at the *input* of the SISO module is evaluated using (5), which, for an *i.i.d.* binary sequence, reduces to [6]

$$I_A(\sigma_A) = 1 - \int_{\infty}^{\infty} \frac{e^{-(\xi - \sigma_A^2/2)^2/(2\sigma_A^2)}}{\sqrt{2\pi}\sigma_A} \cdot \log_2(1 + e^{-\xi}) d\xi. \quad (6)$$

Clearly, I_A is independent of the corresponding transmitted bits. Thus, it can be precomputed and tabulated.

To obtain the decoder transfer characteristic, a simulation setup shown in Fig. 2(a) is used. By varying σ_A^2 so that I_A ranges from 0 to 1, the decoder transfer characteristic (a plot between I_A and I_D^{out}) is obtained. Similarly, the equalizer transfer characteristic (a plot between I_A and I_E^{out}) of the conventional receiver can be obtained by running a simulation in Fig. 2(b), where the data bits $\{c_k\}$ are randomly generated without the encoder. Hence, the EXIT chart is realized by combining the transfer characteristics of the equalizer and the decoder into a single diagram where the axes of the decoder are swapped. The exchange of the mutual information, I_E^{out} and I_D^{out}, over the iterations in the complete receiver can be visualized as a system trajectory in the EXIT chart [6].

To obtain the equalizer transfer characteristic of the NBM scheme, the simulation setup in Fig. 2(b) needs to be modified as illustrated in Fig. 3, where $\lambda_k = L_D(c_k) + L_E'(c_k)$ is the LLR at the output of the SISO decoder. Given $\{\lambda_k\}$, the soft
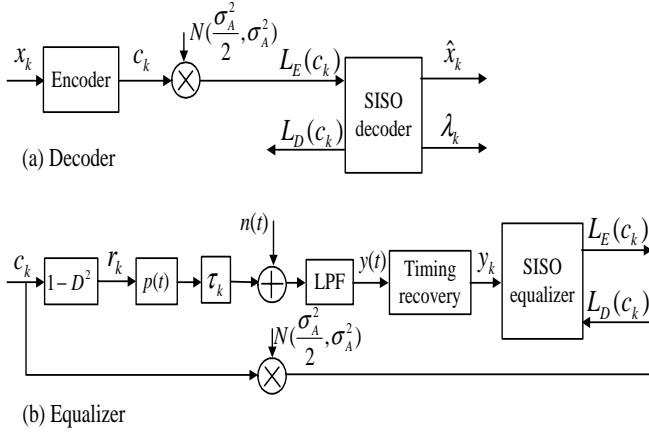
(a) Decoder

(b) Equalizer

Fig. 2. Simulation setup for generating the mutual information transfer characteristics of the conventional receiver for (a) the decoder and (b) the equalizer.
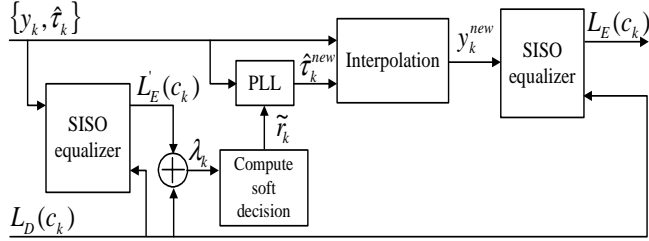

Fig. 3. Simulation setup for generating the equalizer transfer characteristic of the NBM scheme.

estimates $\{\tilde{r}_k\}$ for the PR-IV channel can be expressed as

$$\tilde{r}_k = E[r_k|\{\lambda_k\}] = \frac{2(e^{\lambda_k} - e^{\lambda_{k-2}})}{(1 + e^{\lambda_k})(1 + e^{\lambda_{k-2}})}. \quad (7)$$

The second PLL uses these soft estimates and the original samples $\{y_k\}$ to output an improved set of the sampling phase offsets, $\{\hat{\tau}_k^{new}\}$, which will be employed to resample $\{y_k\}$ by means of interpolation. In this paper, a 21-tap sinc interpolation filter is employed. A new set of the samples $\{y_k^{new}\}$, given by

$$y_k^{new} = \sum_{i=k-10}^{k+10} y_i p(kT - iT - \hat{\tau}_i + \tau_k^{new}), \quad (8)$$

is then used to compute the equalizer transfer characteristic.

Finally, for the equalizer transfer characteristic of per-survivor iterative timing recovery, we only replace the timing recovery block and the SISO equalizer in Fig. 2(b) with a PSP-BCJR module and then run a simulation to generate the equalizer transfer characteristic as described earlier.

B. Predicted Bit-Error Rate

As shown in (6), there is one-to-one mapping between σ_A^2 and I_A. Therefore, if we define [6]

$$J(\sigma) := I_A(\sigma_A = \sigma) \quad (9)$$

with

$$\lim_{\sigma \to 0} J(\sigma) = 0 \ \text{ and } \ \lim_{\sigma \to \infty} J(\sigma) = 1, \ \text{ for } \sigma > 0, \quad (10)$$

it is true that

$$\sigma_A = J^{-1}(I_A) \quad (11)$$

because I_A is monotonically increasing in σ_A and thus reversible [6]. Note that the relationship in (11) is also valid for the mutual information at the output of both the equalizer and the decoder [6].

Consequently, we can predict the BER performance evaluated at the SISO decoder output, whose LLR is given by $\lambda_k = L_E(c_k) + L_D(c_k)$, as follows. Assuming that λ and L are Gaussian distributed and independent, we can write

$$\sigma_\lambda^2 = \sigma_E^2 + \sigma_D^2, \quad (12)$$

where

$$\sigma_E^2 \approx (J^{-1}(I_D^{in}))^2, \quad (13)$$
$$\sigma_D^2 \approx (J^{-1}(I_D^{out}))^2, \quad (14)$$

and $I_D^{in} = I_E^{out}$.

For simplicity, we also assume that $\lambda \sim \mathcal{N}(\sigma_\lambda^2/2, \sigma_\lambda^2)$. With the complementary error function [12], the error probability at the output of the SISO decoder, P_e, can then be expressed as

$$
\begin{aligned}
P_e & \approx \frac{1}{2} \operatorname{erfc}\left(\frac{\sigma_\lambda}{2\sqrt{2}}\right) \\
& \approx \frac{1}{2} \operatorname{erfc}\left(\frac{\sqrt{(J^{-1}(I_D^{in}))^2 + (J^{-1}(I_D^{out}))^2}}{2\sqrt{2}}\right). \quad (15)
\end{aligned}
$$

IV. NUMERICAL RESULTS

Consider a rate-8/9 system in which a block of 3640 message bits is encoded by a regular $(3, 27)$ low-density parity-check (LDPC) code [13], resulting in a coded block length of 4095 bits. The parity-check matrix has 3 ones in each column and 27 ones in each row. With an LDPC outer code, the interleaver is not needed. The SISO equalizer is implemented based on the BCJR algorithm [4], whereas the SISO decoder is implemented based on the message passing algorithm [13] with 5 internal iterations. The PLL gain parameters for different iterative timing recovery schemes were optimized based on minimizing the RMS timing error, $\sigma_\epsilon = \sqrt{E[(\tau_k - \hat{\tau}_k)^2]}$, at a per-bit SNR, E_b/N_0, of 5 dB. Each point in the EXIT chart is obtained by averaging the extrinsic output pdf's over $N = 1000$ blocks according to

$$\overline{p(l|C = \pm 1)} = \frac{1}{N} \sum_{i=1}^{N} p_i(l|C = \pm 1). \quad (16)$$

Note that because cycle slipping [11] is a major performance limiting factor, which causes I_E^{out} to drop drastically, we then consider *only* the data blocks that contain no cycle slip in simulation. With this assumption, we can demonstrate that all benefits obtained from the EXIT chart analysis are still valid for iterative timing recovery schemes.

We first consider the system at $E_b/N_0 = 5$ dB with a moderate random walk parameter $\sigma_w/T = 0.5\%$, which implies a low probability of occurrence of a cycle slip. The
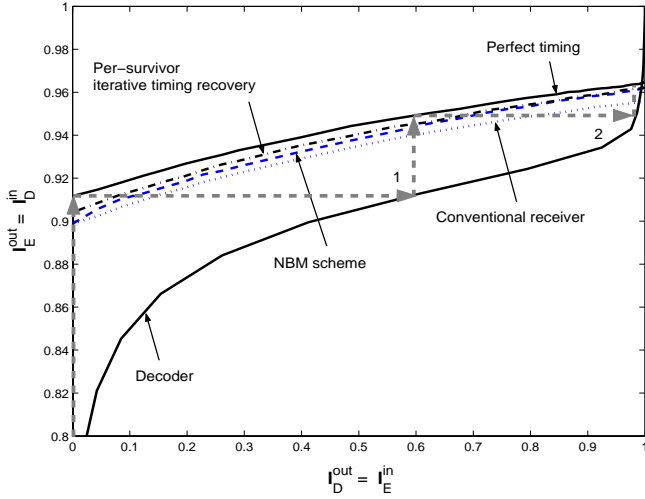
Fig. 4. The mutual information transfer characteristics of different iterative timing recovery schemes at $E_b/N_0 = 5$ dB and $\sigma_w/T = 0.5\%$.
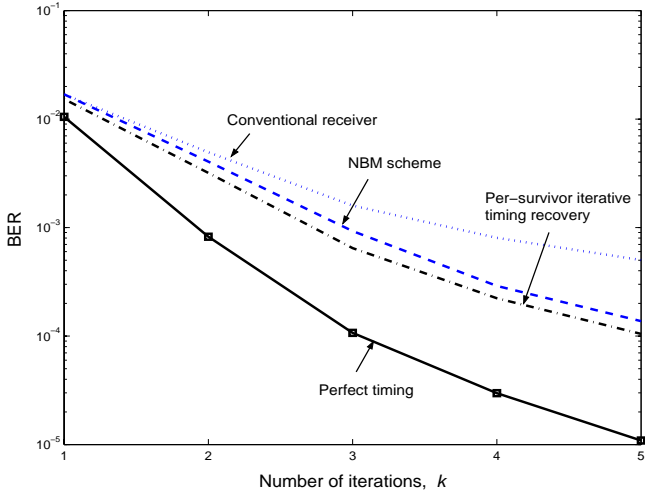

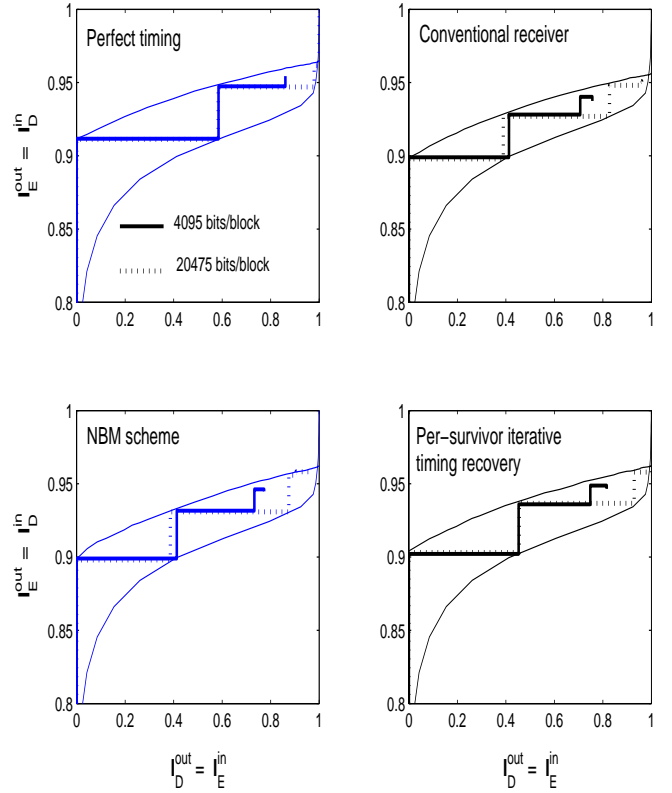Fig. 5. BER performance comparison at $E_b/N_0 = 5$ dB and $\sigma_w/T = 0.5\%$.

Fig. 6. System trajectories at $E_b/N_0 = 5$ dB and $\sigma_w/T = 0.5\%$. The solid lines are based on the coded block length of 4095 bits, whereas the dashed lines are based on the coded block length of 20475 bits

α's for the conventional receiver, the NBM algorithm, and per-survivor iterative timing recovery are 0.0053, 0.0053, and 0.0028, respectively. Fig. 4 depicts the EXIT chart of different iterative timing recovery schemes, and its corresponding BER plot is given in Fig. 5. The dashed arrows in Fig. 4 describe the system trajectory of the system with perfect timing (i.e., a conventional receiver that uses $\hat{\tau}_k = \tau_k$ to sample $y(t)$). The iteration starts at the $(0, 0)$ point where the equalizer has no *a priori* information so that $I_E^{in} = 0$, and ends at the point where the equalizer transfer characteristic intersects the decoder one. Note that we refer to the first pass through the decoder as the first iteration.

As expected, for a given number of iterations, the system with perfect timing yields the largest I_D^{out} or, equivalently, the lowest BER, followed by per-survivor iterative timing recovery, the NBM scheme, and the conventional receiver. Apparently, the higher the I_D^{out}, the smaller the BER.

We also show the system trajectory of different schemes with two different coded block lengths in Fig. 6. Clearly, the larger the coded block length, the better the system trajectory matches the transfer characteristics. This is because the EXIT chart analysis assumes that all LLRs are independent, and thus it is valid only for an infinite block length [6].

Next, we consider the system at $E_b/N_0 = 5$ dB with a severe random walk parameter $\sigma_w/T = 1\%$, which implies a high probability of occurrence of a cycle slip. The α's for the conventional receiver, the NBM scheme, and per-survivor iterative timing recovery are 0.0103, 0.0103, and 0.006, respectively. The EXIT chart of different iterative timing recovery schemes is depicted in Fig. 7, and its corresponding BER plot is shown in Fig. 8. Clearly, there is a big performance gap between per-survivor iterative timing recovery and the NBM scheme. This implies that per-survivor iterative timing recovery outperforms the NBM scheme when the timing error is large (same conclusion as presented in [2]).

Finally, Fig 9 plots the SNR (in dB) required to achieve BER $= 10^{-4}$ at the decoder output at the 2nd iteration as a function of σ_w/T's. The solid lines are the predicted BER computed from (15), whereas the dashed lines are the BER obtained by simulating data transmission over the complete iterative receiver. As expected, per-survivor iterative timing recovery performs better than the NBM scheme, and both outperforms the conventional receiver, especially when the timing error is severe. Obviously, there is a big gap between the predicted BER and the simulated one. However, we observed that this
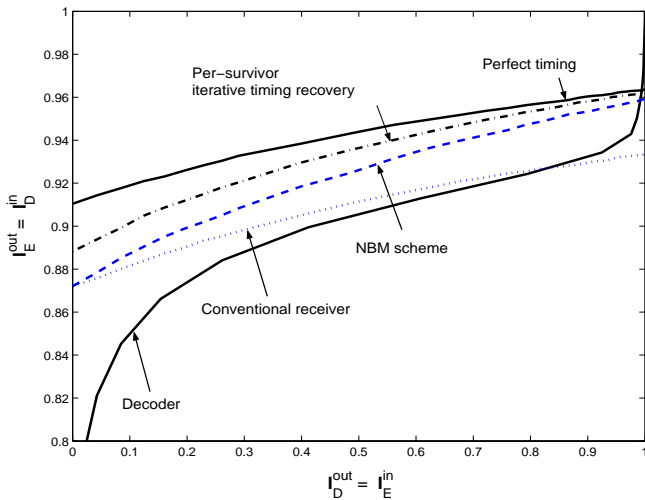
Fig. 7. The mutual information transfer characteristics of different iterative timing recovery schemes at $E_b/N_0 = 5$ dB and $\sigma_w/T = 1\%$.

Fig. 9. SNR required to achieve BER = 10^{-4} at the decoder output at the 2nd iteration as a function of σ_w/T's.
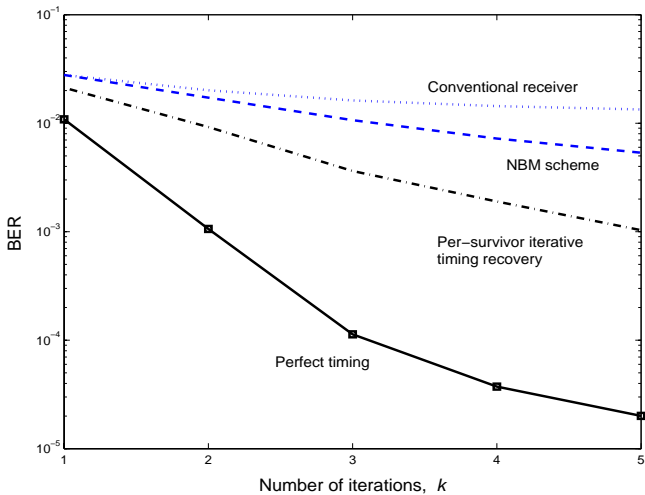

Fig. 8. BER performance comparison at $E_b/N_0 = 5$ dB and $\sigma_w/T = 1\%$.

gap gets smaller when using a larger coded block length. Again, this is because the EXIT chart analysis is based on the assumption that the coded block length is infinite [6]. Nonetheless, for a small coded block length, we can use the predicted BER as a practical bound on the achievable performance.

In addition, we also observed that all benefits obtained from the EXIT chart analysis as investigated in [6] (e.g., finding the SNR threshold, evaluating the effect of the different constituent codes, etc.) are also valid for iterative timing recovery schemes, assuming that there is no cycle slip. Therefore, it is sufficient to use the EXIT chart as a convenient measure to compare the performance of iterative timing recovery schemes because it requires much less simulation time than a BER criterion.

V. CONCLUSION

We showed that the EXIT chart analysis can still be used to predict the performance of iterative timing recovery schemes,
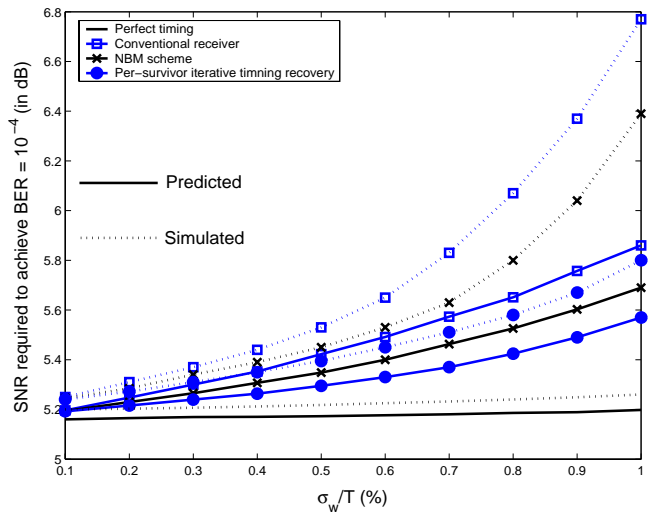
assuming that there is no cycle slip in a system. The result predicted by the EXIT chart coincides with that obtained by simulating data transmission over the complete iterative receiver. It is clear that for a given number of turbo iterations, the higher the mutual information at the decoder output, the lower the BER. As a result, the EXIT chart can be equivalently used instead of BER as a measure to compare the performance of different iterative timing recovery schemes.

REFERENCES

[1] A. R. Nayak, J. R. Barry, and S. W. McLaughlin, "Joint timing recovery and turbo equalization for coded partial response channels," *IEEE Trans. Magnetics*, vol. 38, no. 5, pp. 2295-2297, September 2003.

[2] P. Kovintavewat, J. R. Barry, M. F. Erden, and E. Kurtas, "Per-survivor iterative timing recovery for coded partial response channels," to appear in *Globecom 2004*, Dallas, Texas, USA, November 28 – December 3, 2004.

[3] T. Souvignier, A. Friedmann, M. Oberg, P. Siegel, R. Swanson, and J. Wolf, "Turbo decoding for PR4: parallel vs. serial concatenation," in *Proc. of ICC'99*, vol. 3, pp. 1638-1642, 1999.

[4] L. R. Bahl, J. Cocke, F. Jelinek and J. Raviv, "Optimal decoding of linear codes for minimizing symbol error rate," *IEEE Trans. Inform. Theory*, vol. IT-20, pp. 248-287, March 1974.

[5] R. Raheli, A. Polydoros, and C. K. Tzou,"The principle of per-survivor processing: a general approach to approximate and adaptive MLSE," in *Proc. of GLOBECOM'91*, pp. 11.3.1-11.3.6, December 1991.

[6] S. ten Brink, "Convergence behavior of iteratively decoded parallel concatenated codes," *IEEE Trans. Commun.*, vol. 49, no. 10, pp. 1727-1737, October 2001.

[7] C. Heegard and S. B. Wicker, *Turbo Coding.* Boston, Massachusetts: Kluwer Academic Publishers, 1999.

[8] M. Tüchler, R. Koetter, and A. C. Singer, "Turbo equalization: principles and new results," *IEEE Trans. Commun.*, 50(5):754-767, May 2002.

[9] R. Otnes and M. Tüchler, "EXIT chart analysis applied to adaptive turbo equalization," in *Proc. Nordic Signal Processing Symposium*, on board Hurtigruten, Norway, October 2002.

[10] A. N. D' Andrea, U. Mengali, and G. M. Vitteta, "Approximate ML decoding of coded PSK with no explicit carrier phase reference," *IEEE Trans. Commun.*, vol. 42, pp. 1033-1039, Feb./Mar./Apr. 1994.

[11] J. W. M. Bergmans, *Digital baseband transmission and recording.* Boston, Massachusetts: Kluwer Academic Publishers, 1996.

[12] J. R. Barry, E. A. Lee, and D. G. Messerschmitt, *Digital Communication.* 3rd edition, Boston, Massachusetts: Kluwer Academic Publishers, 2003.

[13] R. Gallager, "Low-density parity-check codes," *IRE Trans. Inform. Theory*, vol. IT-8, pp. 21-28, January 1962.